

[Pd₃Sn₈Bi₆]⁴⁻: A 14-Vertex Sn/Bi Cluster Embedding a Pd₃ Triangle

Felicitas Lips,[†] Rodolphe Clérac,^{‡,§} and Stefanie Dehnen^{*,†}

[†]Fachbereich Chemie and Wissenschaftliches Zentrum für Materialwissenschaften, Philipps-Universität Marburg, Hans-Meerwein-Strasse, D-35032 Marburg, Germany

[‡]CNRS, UPR 8641, Centre de Recherche Paul Pascal (CRPP), Equipe “Matériaux Moléculaires Magnétiques”, 115 avenue du Dr. Albert Schweitzer, Pessac, F-33600, France

[§]Université de Bordeaux, UPR 8641, Pessac, F-33600, France

S Supporting Information

ABSTRACT: The endohedral cluster anion [Pd₃Sn₈Bi₆]⁴⁻ crystallizes as its K([2.2.2]crypt)⁺ salt **1** upon reaction of [K([2.2.2]crypt)]₂[Sn₂Bi₂]·*en* and Pd(dppe)₂ in 1,2-diaminoethane (*en*)/toluene and incorporates a complete Pd₃ triangular cluster within a medium-size 14-vertex cage of Sn and Bi atoms. **1** was characterized by a combination of single crystal diffraction, ESI mass spectrometry, elemental analysis, and magnetic measurements. According to quantum chemical investigations, the Pd₃ triangle interacts only weakly with the Sn/Bi cluster shell despite the relatively small cavity inside the cage.

Research activity in the field of main group element cages comprising transition metal atoms,¹ so-called “intermetalloid clusters”, is rapidly expanding.² The high interest in these clusters, that represent a modern extension of Zintl phase chemistry, is based on their uncommon geometric and electronic structures, their similarities to fullerenes,³ and intriguing gas phase chemistry.⁴ Furthermore, intermetalloid clusters are discussed as potential building blocks for cluster assembled nanomaterials.⁵

Only a limited number of intermetalloid clusters are known that encase more than one—namely, two or three—interstitial transition metal atoms that either form a dumbbell in [Pt₂@Sn₁₇]⁴⁻,⁶ [Pd₂@Sn₁₈]⁴⁻,⁷ and [Pd₂@Ge₁₈]⁴⁻,⁸ or a trimeric filament in [Ni₃@(Ge₉)₂]⁴⁻.⁹ In contrast, in alloy-like clusters such as [Ni₃Sb₁₇]⁴⁻,^{10a} [Pd₇As₁₆]⁴⁻,^{10b} or [Zn₉Bi₁₁]⁵⁻,¹¹ most of the transition metal atoms contribute to the surface affording unusual shapes and complicated electronic situations.

Herein we report on [Pd₃Sn₈Bi₆]⁴⁻ that uniquely accommodates a triangular Pd₃ cluster completely inside a medium-size, 14-vertex Sn/Bi cage. As a result of the large ratio of interstitial/surface atoms (3:14), the Pd₃ cluster is tightly fixed inside the Sn/Bi shell, without exhibiting significant bonding interactions with the latter.

[K([2.2.2]crypt)]₄[Pd₃Sn₈Bi₆]·0.6*en* (**1**) is obtained by the reaction of [K([2.2.2]crypt)]₂[Sn₂Bi₂]·*en*¹² with Pd(dppe)₂,¹³ as extremely air-sensitive black rhombus-like crystals (Scheme 1, Supporting Information).

The cluster anion in **1** is composed of a bicapped trigonal prism of Sn atoms with all three rectangular faces centered by one of the three Pd atoms and capped by one of three Bi₂ dumbbells in plane with the Pd₃ unit. The Pd–Pd distances within the

embedded [Pd₃] cluster in **1** (2.756(2)–2.774(2) Å) are at the upper limit of reported Pd–Pd bond lengths. Whereas the Pd–Pd distances are smaller in Pd₃(CN-*c*-Hx)₆ (2.651 Å),¹⁴ they are very similar within the Pd₃ units of ditropylium halides (2.755–2.773 Å)¹⁵ or sandwich complexes with arenes (2.702–2.830 Å),¹⁶ all indicating stronger Pd–Pd interactions than in [Pd₂@Ge₁₈]⁴⁻ (2.831 Å).⁸

The incorporation of a complete transition metal cluster within a main group metal cage is unprecedented, even though a triangular unit represents the smallest possible cluster type. Indeed, a larger cluster inside a main group atom cage has so far only been reported for the outstanding example [As@Ni₁₂@As₂₀]³⁻.¹⁷ However, the situation is different here, since the cavity inside an As₂₀ cage does not allow for accommodation of 12 Ni atoms: the transition metal atoms are rather viewed as contributing to a deltahedral 32-atom shell, but shifted slightly below the pentagonal faces of the As₂₀ pentagon-dodecahedron to form an “inner” icosahedron.

The ratio of K/Pd/Sn/Bi = 4:3:8:6 was confirmed by a combination of electrospray ionization mass spectrometry (ESI-MS), elemental analyses (EDX and microanalysis) and magnetic measurements indicating a diamagnetic anion in **1** (Figure S3, Supporting Information). The ESI-MS investigations of single crystals of **1** dissolved in dimethylformamide (Figure 2) revealed the [Pd₃Sn₈Bi₆]⁻ species to be stable in solution. Additional ESI-MS experiments of the reaction mixture indicate only a few [Sn_{*x*}Bi_{*y*}] fragments to be present beside the predominant nine-atom cage attached to a single Pd atom, [PdSn₆Bi₃]⁻ (Supporting Information). A similar species, [NiSn₆Bi₃]⁻, was also detected in the reaction mixture during the formation of [Ni₂Sn₇Bi₅]³⁻,¹⁸ thus this precursor species might play a key role at the formation of the title compound. Still, the complicated fragmentation/rearrangement pathways are unclear and wait for further elucidation by comprehensive experimental and theoretical studies.

In all compounds with binary cluster shells reported so far, [Sn₂Sb₅(ZnPh)₂]³⁻,¹⁹ [Zn₆Sn₃Bi₈]⁴⁻,²⁰ [Ni₂Sn₇Bi₅]³⁻,¹⁸ and [Eu@Sn₆Bi₈]⁴⁻,²¹ the assignment of Sn/Sb or Sn/Bi atomic positions suffered from statistical and/or rotational disorder which was more distinct for increasing spherical cluster shells. In contrast, the topology of the anion in **1**, that features a higher anisotropy of the cluster shell, seems to allow for a specific,

Received: April 11, 2011

Published: August 11, 2011

Scheme 1. Synthesis and Crystallization of Compound 1

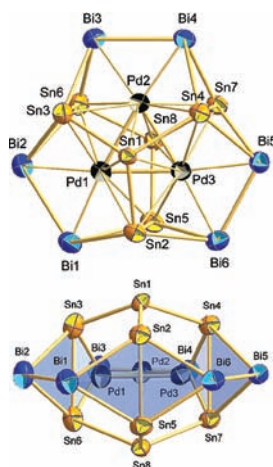
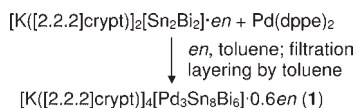


Figure 1. Thermal ellipsoid plot of the molecular cluster anion $[\text{Pd}_3\text{Sn}_8\text{Bi}_6]^{4-}$ in **1**. Selected bond lengths /Å: Sn1–Sn2, 4, 2.910(2)–2.944(2); Sn8–Sn5–7, 2.898(2)–2.917(2); Sn2–4–Sn5–7, 3.188(2)–3.261(2); Sn2–4–Bi1–6, 3.041(2)–3.073(2); Sn5–7–Bi1–6, 3.020(2)–3.094(2), Bi–Bi, 3.124(2)–3.150(2); Pd–Pd, 2.756(2)–2.774(2); Pd–Sn1,8, 2.963(2)–3.025(2); Pd–Sn2–4, 2.868(2)–2.917(2); Pd–Sn5–7, 2.870(2)–2.920(2), Pd–Bi, 2.728(2)–2.752(2). Angles of the nonplanar butterfly type Sn_2Bi_2 four-membered rings: 62.6(1)–65.1(1)°/110.2(1)–117.8(1)°.

“ordered” Sn/Bi atomic distribution in accordance with quantum chemical calculations. Simultaneous optimization of the geometric and electronic structure of the 292 possible isomers of $[\text{Pd}_3\text{Sn}_8\text{Bi}_6]^{4-}$, using DFT²² methods of the program system Turbomole²³ and the COSMO model for charge compensation,²⁴ revealed the presented isomer (Figure 1) to be by 18–165 $\text{kJ}\cdot\text{mol}^{-1}$ more stable than all other isomers (see Supporting Information).

The topology of the 14-vertex main group atom shell was recently observed in two further isolated clusters, however with certain differences to the anion in **1**. The cluster anion in $\text{Ge}_{14}[\text{Ge}(\text{SiMe}_3)_3]_5\text{Li}_3(\text{THF})_6$ ²⁵ is empty and is decorated by five external ligands. The endohedral cluster anion $[\text{Eu}^{\text{II}}@ \text{Sn}_6\text{Bi}_8]^{4-21}$ differs in the number of Sn and Bi atoms, the nature and number of interstitial atoms, and possesses a more spherical structure; this indicates the high synthetic potential of the binary precursor $[\text{Sn}_2\text{Bi}_2]^{2-}$, allowing for a structural and electronic adjustment of the 14-atom cage to the demands of the respective inner moiety in the ternary system. The three examples are compared in Figure 3.

The structural features of the two cited 14-vertex cluster anions correlate well with their electron numbers: the spherical shape of $[\text{Eu}^{\text{II}}@ \text{Sn}_6\text{Bi}_8]^{4-}$ is in perfect agreement with a formal pseudoelement $[(\text{Sn}^-)_6\text{Bi}_8]^{6-} = [\text{Bi}_{14}]$ shell, with exclusively three-bonded atoms; accordingly, the distortion toward an oblate spheroid observed in $\text{Ge}_{14}[\text{Ge}(\text{SiMe}_3)_3]_5\text{Li}_3(\text{THF})_6$ via formation of three Ge–Ge bonds corresponds with a formal $[(\text{Ge}^-, \text{Ge}^-)_8]^{8-}$ core. In contrast, the electron number–structure

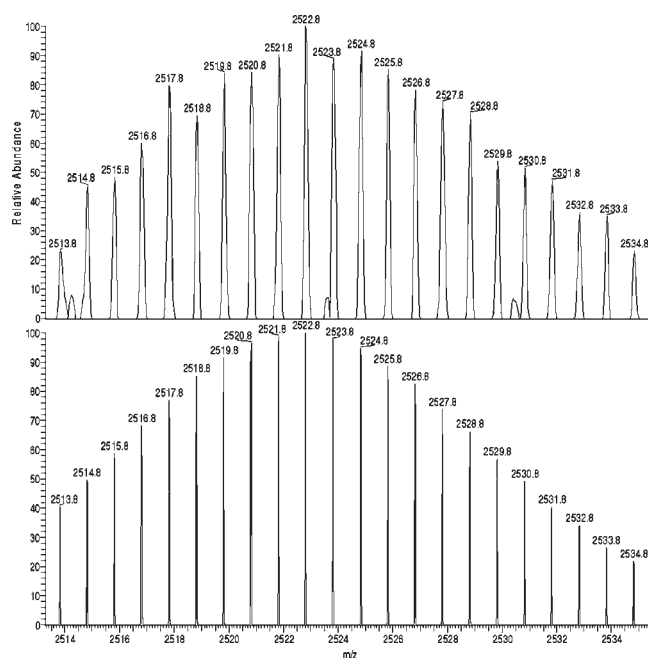


Figure 2. Isotope pattern of the $[\text{Pd}_3\text{Sn}_8\text{Bi}_6]^-$ species in the ESI mass spectrum of **1**, measured (top) and simulated (bottom).

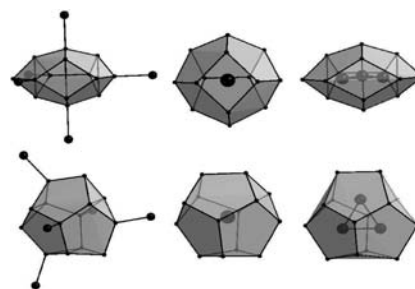


Figure 3. Side views (top) and top views (bottom) of 14-vertex cluster anions (from left): $[\text{Ge}_{14}[\text{Ge}(\text{SiMe}_3)_3]_5]^{3-}$ (without SiMe_3 ligands),^{25a} $[\text{Eu}^{\text{II}}@ \text{Sn}_6\text{Bi}_8]^{4-21}$ and $[\text{Pd}_3\text{Sn}_8\text{Bi}_6]^{4-}$ in **1** (this work).

correlation is not trivial in the anion of **1**. This problem occurred also for other Group 10 endohedral cluster anions. In the deltahedral cluster $[\text{Ni}_2\text{Sn}_7\text{Bi}_5]^{3-}$,¹⁸ for instance, accordance with the pseudoelement concept²⁶ or with Wade-Mingos rules²⁷ failed by two missing or extra electrons, respectively.

Regarding the interstitial Pd_3 unit in the cluster anion in **1** as neutral and neglecting any Pd–Sn/Bi interactions, six three-bonded Bi^0 atoms, six four-bonded Sn^0 atoms, and two three-bonded Sn^- atoms would add up to a total charge of -2 , which does not agree with the presence of four counter-cations per formula unit. However, the oblate cluster topology seems to be stable for a range of total valence electron numbers (VE) in the case of empty clusters: (i) a hypothetical C_{14} fullerene (56 VE),²¹ (ii) the global minimum structure of $[\text{Ge}_{14}]^{4-}$, according to DFT calculations by King and co-workers (60 VE),²⁸ (iii) the formal $[\text{Ge}_{14}]^{8-}$ core of $\text{Ge}_{14}[\text{Ge}(\text{SiMe}_3)_3]_5\text{Li}_3(\text{THF})_6$ (64 VE). The differences in the electron numbers are reflected in different average bond lengths. Therefore, the $[\text{Sn}_8\text{Bi}_6]^{4-}$ shell in **1** (66 VE) might just extend this range by another two electrons. This situation is represented by the formula “ $\{[\text{Pd}_3]^0@[\text{Sn}_8\text{Bi}_6]^{4-}\}^{4-}$ ”, denoted as the “0 + 4” model in the following.

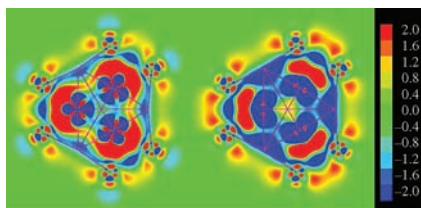


Figure 4. Difference electron densities $\Delta\rho(“0 + 4”) = \rho\{[\text{Pd}_3\text{Sn}_8\text{Bi}_6]^{4-}\} - \{\rho[\text{Pd}_3] + \rho([\text{Sn}_8\text{Bi}_6]^{4-})\}$ (left) or $\Delta\rho(“2 + 2”) = \rho\{[\text{Pd}_3\text{Sn}_8\text{Bi}_6]^{4-}\} - \{\rho([\text{Pd}_3]^{2-}) + \rho([\text{Sn}_8\text{Bi}_6]^{2-})\}$ (right), based on DFT calculations of the ternary cluster anion and the according fragments on the cluster atomic positions. Electron densities are drawn from 2×10^{-3} a.u. (red) to -2×10^{-3} a.u. (blue).

An alternative view involves the Pd_3 cluster in bonding interactions, leading to the formula “ $\{[\text{Pd}_3]^{2-} @ [\text{Sn}_8\text{Bi}_6]^{2-}\}^{4-}$ ”. This “2 + 2” model describes a charged cluster $[\text{Pd}_3]^{2-}$ inside an electron-precise $[(\text{Sn}^-)_2\text{Sn}_6\text{Bi}_8]^{2-}$ shell that accords perfectly with the pseudoelement concept. Indeed, as previously reported by Ahlrichs and co-workers,²⁹ a neutral Pd_3 cluster possesses a very small highest occupied molecular orbital–lowest unoccupied molecular orbital (HOMO–LUMO) gap (0.12 eV), which suggests an easy acceptance of two further electrons, although the formulation of an “anion within an anion” is questionable.

Comprehensive quantum chemical studies were performed to explore the bonding situation in the uncommon $[\text{Pd}_3\text{Sn}_8\text{Bi}_6]^{4-}$ anion in **1** and to judge on the accordance with either the “0 + 4” or the “2 + 2” model.

Calculation of natural charges by natural population analysis (NPA,³⁰ see Supporting Information) rather supports the “0 + 4” model. A nearly neutral Pd_3 ring (total charge -0.24) is observed beside a charge of -0.34 at each of the Bi atoms and the two Sn caps, and a charge of -0.17 at each of the six remaining Sn atoms. Thus, unlike the suggestion according to the “2 + 2” model, the Bi atoms and the two capping Sn atoms possess the same charge, together holding 70% of the total charge of the anion. Only the larger charge at the Sn caps in comparison with the atoms of the Sn_6 prism rudimentarily refers to the idea of the pseudoelement concept with charged versus neutral Sn atoms.

By optimization of the structures of the respective fragments, Pd_3 and $[\text{Sn}_8\text{Bi}_6]^{4-}$, or $[\text{Pd}_3]^{2-}$ and $[\text{Sn}_8\text{Bi}_6]^{2-}$, we intended to simulate the two models for comparison with the calculated $[\text{Pd}_3\text{Sn}_8\text{Bi}_6]^{4-}$ anion. However, geometric parameters (Table S6) as well as molecular orbitals—delocalized (MOs,³¹ Supporting Information, Figures S11, S12) or localized (LMOs,³² Figure S13)—do not allow for the declaration of one of the models to better represent the situation in the ternary cluster. One might use this result to claim a mixture of both variants to be present in the $[\text{Pd}_3\text{Sn}_8\text{Bi}_6]^{4-}$ anion; nevertheless, it should be noted that deviations of the isolated fragments’ geometries from the original atomic positions in $[\text{Pd}_3\text{Sn}_8\text{Bi}_6]^{4-}$ affect the bonding in the fragments and might thus hamper a reasonable comparison.

To avoid this, we calculated difference electron densities that are solely based on the geometry of the ternary cluster anion. For this, total densities were calculated for $[\text{Pd}_3\text{Sn}_8\text{Bi}_6]^{4-}$ as well as for the fragments cut out of the cluster without further optimization of the structures. Subtraction of the sum of the total densities, obtained either for the “0 + 4” or the “2 + 2” model, from the total density of $[\text{Pd}_3\text{Sn}_8\text{Bi}_6]^{4-}$ resulted in the pictures provided in Figure 4. While red clouds indicate excess electron density at the respective grid point of $[\text{Pd}_3\text{Sn}_8\text{Bi}_6]^{4-}$, blue clouds

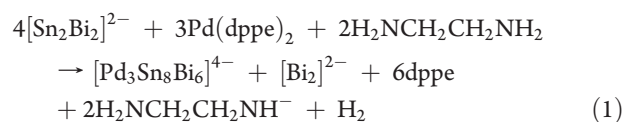
represent a lower electron density in $[\text{Pd}_3\text{Sn}_8\text{Bi}_6]^{4-}$ in comparison with the electron density sum of the fragments.

Figure 4 shows clearly that neither of the two fragment models exactly reproduces the electron density in the ternary cluster anion. However, two major things can be gathered from the pictures. First, the “0 + 4” model (Figure 4, left) shows both slight excess and slight deficit of the electron density on the cluster surface, whereas the “2 + 2” model (Figure 4, right) shows only excess electron density. This indicates a better balanced distribution of the electron densities in the “0 + 4” model with respect to the ternary anion. Second, subtraction of the “2 + 2” model from the cluster results in a much more significant deficit of electron density at the Pd atoms than does a subtraction of the “0 + 4” variant, indicative for a too high charge assignment by the $[\text{Pd}_3]^{2-}$ model. Integration of the excess and deficit electron densities observed for each of the differences—as an indication for the deviation of the models from the situation within the ternary cluster anion—results in a total of four electrons for the “0 + 4” model and five electrons for “2 + 2”.

The computational studies demonstrate that neither “ $\{[\text{Pd}_3]^{0} @ [\text{Sn}_8\text{Bi}_6]^{4-}\}^{4-}$ ” nor “ $\{[\text{Pd}_3]^{2-} @ [\text{Sn}_8\text{Bi}_6]^{2-}\}^{4-}$ ” perfectly represent the real charge distribution and thus the bonding situation in the anion in **1**. However, a clear tendency toward the first model is suggested by the assignment of natural charges or, accordingly, the inspection of the electron density distribution.

Comparison with previous results leads to the conclusion that formal assignment of charges according to the pseudoelement concept is possible if the clusters show dominantly ionic interactions of the interstitial metal atom(s) with the cluster shell, such as observed in $[\text{Eu}(\text{II}) @ \text{Sn}_6\text{Bi}_8]^{4-}$, but is not appropriate for weak or more covalent interactions like in $[\text{Ni}_2\text{Sn}_7\text{Bi}_5]^{3-}$ or in the anion in **1**. The latter are characterized by cluster orbital formation (Figures S11, S12) including the embedded atom(s), and thus by a more intermetallic nature.

Another question concerns the formation of **1**. This is at least as difficult to answer as for binary intermetallic clusters. So far, only some of the latter have been explored with respect to their formation, like $[\text{Ir} @ \text{Sn}_{12}]^{3-}$,³³ $[\text{Ni}_3 @ (\text{Ge}_9)_2]^{4-}$,⁹ or $[\text{Eu} @ \text{Sn}_6\text{Bi}_8]$.²¹ Corresponding studies were facilitated by detectable intermediates that point toward a plausible mechanism. In the case of the title compound, the only hint toward an intermediate is a species $[\text{PdSn}_6\text{Bi}_3]^-$ that was observed in the ESI mass spectrum of the reaction solution (Figures S4, S15, and S7). However, it was not possible to isolate or detect further possible precursors, such as “ $[(\text{Sn}_2\text{Bi}_2)\text{Pd}(\text{dppe})]^{2-}$ ”, for instance, which may be involved in the first steps of the cluster formation. According to both experimental and quantum chemical studies, we assume that the cluster was actually formed by condensation of three reactive endohedral clusters with eight or nine main group atoms that are initially formed under release of the detectable byproduct $[\text{Bi}_2]^{2-}$. The condensation steps includes the electron transfer from the intermetallic anion(s) onto *en* molecules under formation of H_2 and the formation of elemental Sn and/or the starting material $[\text{Sn}_2\text{Bi}_2]^{2-}$ (see Supporting Information for details). To sum up, we provide the following reaction scheme:



All products given in eq 1 have been unambiguously confirmed by a variety of experimental findings, except the deprotonated *en*

molecules. However, since we can exclude dppe as the source of H₂ (see Supporting Information), it is plausible to choose *en* as this source, being the most acidic species in the system. Comprehensive quantum chemical studies are currently underway to get even deeper insight into this complicated process and into the formation of ternary intermetallic clusters in general.

In conclusion, we show that a binary-to-ternary synthetic approach enables an extraordinary adjustment of structural and electronic features of a 14-vertex polyhedron to accommodate a Pd₃ ring, resulting in an unprecedented anionic cluster@cluster structure. Common concepts for intracluster bonding fail in the title compound; despite weak interaction with the main group metal shell, the Pd₃ cluster is best approximated as the neutral [Pd₃]^{±0} that is trapped within the comparatively small cavity of an [Sn₈Bi₆]⁴⁻ anion. The stability of the cluster anion was additionally confirmed by ESI mass spectrometry in dimethylformamide (DMF) solution.

■ ASSOCIATED CONTENT

S Supporting Information. Further details on synthesis, X-ray structural analyses, EDX analyses, magnetic measurements, ESI-MS, microanalysis, H₂ detection, NMR studies, and DFT investigations on both the cluster anion in **1** and its formation. This material is available free of charge via the Internet at <http://pubs.acs.org>.

■ AUTHOR INFORMATION

Corresponding Author

dehnen@chemie.uni-marburg.de

■ ACKNOWLEDGMENT

This work was supported by the Fonds der Chemischen Industrie FCI (Chemiefonds-Stipendium for F.L.), the Deutsche Forschungsgemeinschaft (DFG), the University of Bordeaux, the Région Aquitaine, GIS Advanced Materials in Aquitaine (COMET Project) and the CNRS. We are grateful to Dr. U. Linne and J. Bamberger for ESI-MS measurements, to PD Dr. F. Weigend for calculation of the difference electron densities, and M. Hołyńska for her tremendous help with the crystal structure refinement.

■ REFERENCES

- (1) (a) Scharfe, S.; Kraus, F.; Stegmaier, S.; Schier, A.; Fässler, T. F. *Angew Chem. Int. Ed.* **2011**, *50*, 3630–3670. (b) Scharfe, S.; Fässler, T. F. *Phil. Trans. R. Soc. London, Ser. A* **2010**, *368*, 1265–1284. (c) Sevov, S. C. In *Tin Chemistry: Fundamentals, Frontiers, and Applications*; Davies, A. G., Gielen, M., Pannell, K. H., Tiekink, R. T., Eds.; John Wiley & Sons Ltd: Chichester, UK, 2008; p 138. (d) Sevov, S. C.; Goicoechea, J. M. *Organometallics* **2006**, *25*, 5678–5692.
- (2) Fässler, T. F.; Hoffmann, S. D. *Angew. Chem., Int. Ed.* **2004**, *43*, 6242–6247.
- (3) (a) Cui, L.-F.; Huang, X.; Wang, L.-M.; Li, J.; Wang, L.-S. *Angew. Chem., Int. Ed.* **2007**, *46*, 742–745. (b) Fässler, T. F. *Angew. Chem., Int. Ed.* **2001**, *40*, 4161–4165.
- (4) (a) Grubisic, A.; Ko, Y. J.; Wang, H.; Bowen, K. H. *J. Am. Chem. Soc.* **2009**, *131*, 10783–10790. (b) Dognon, J. P.; Clavaguéra, C.; Pyykkö, P. *Angew. Chem., Int. Ed.* **2007**, *46*, 1427–1430.
- (5) (a) Korber, N. *Angew. Chem., Int. Ed.* **2009**, *48*, 3216–3217. (b) Fässler, T. F. *Angew. Chem., Int. Ed.* **2007**, *46*, 2572–2575. (c) Guloy, A. M.; Ramlau, R.; Tang, Z.; Schnelle, W.; Baitinger, M.; Grin, Y. *Nature*

- 2006**, *443*, 320–323. (d) Kanatzidis, M. G.; Armatas, G. S. *Science* **2006**, *313*, 817–820. (e) Sun, D.; Riley, A. E.; Cadby, A. J.; Richmann, E. K.; Korlann, S. D.; Tolbert, S. H. *Nature* **2006**, *441*, 1126–1130.
- (6) Kesanli, B.; Halsig, J. E.; Zevalij, P.; Fettinger, J. C.; Eichhorn, B. W. *J. Am. Chem. Soc.* **2007**, *129*, 4567–4574.
- (7) (a) Sun, Z.-M.; Xiao, H.; Li, J.; Wang, L.-S. *J. Am. Chem. Soc.* **2007**, *129*, 9560–9561. (b) Kocak, F. S.; Zevalij, P.; Lam, Y.-F.; Eichhorn, B. W. *Inorg. Chem.* **2008**, *47*, 3515–3520.
- (8) Goicoechea, J. M.; Sevov, S. C. *J. Am. Chem. Soc.* **2005**, *127*, 7676–7677.
- (9) Goicoechea, J. M.; Sevov, S. C. *Angew. Chem., Int. Ed.* **2005**, *44*, 4026–4028.
- (10) (a) Moses, M. J.; Fettinger, J. C.; Eichhorn, B. W. *Inorg. Chem.* **2007**, *46*, 1036–1038. (b) Moses, M. J.; Fettinger, J. C.; Eichhorn, B. W. *J. Am. Chem. Soc.* **2002**, *124*, 5944–5945.
- (11) Goicoechea, J. M.; Sevov, S. C. *Angew. Chem., Int. Ed.* **2006**, *45*, 5147–5150.
- (12) Critchlow, S. C.; Corbett, J. D. *Inorg. Chem.* **1982**, *21*, 3286–3290.
- (13) dppe = Bis[1,2-bis(diphenylphosphino)ethane].
- (14) Francis, C. G.; Khan, S. I.; Morton, P. R. *Inorg. Chem.* **1984**, *23*, 3680–3681.
- (15) Mulligan, F. L.; Babbini, D. C.; Davis, I. R.; Hurst, S. K.; Nichol, G. S. *Inorg. Chem.* **2009**, *48*, 2798–2710.
- (16) Murahashi, T.; Fujimoto, M.; Kawabata, Y.; Inoue, R.; Ogoshi, S.; Kurosawa, H. *Angew. Chem., Int. Ed.* **2007**, *46*, 5440–5443.
- (17) Moses, M. J.; Fettinger, J. C.; Eichhorn, B. W. *Science* **2003**, *300*, 778–780.
- (18) Lips, F.; Dehnen, S. *Angew. Chem., Int. Ed.* **2011**, *50*, 955–959.
- (19) Lips, F.; Schellenberg, I.; Pöttgen, R.; Dehnen, S. *Chem.—Eur. J.* **2009**, *15*, 12968–12973.
- (20) Lips, F.; Dehnen, S. *Angew. Chem., Int. Ed.* **2009**, *48*, 6435–6438.
- (21) Lips, F.; Clérac, R.; Dehnen, S. *Angew. Chem., Int. Ed.* **2011**, *50*, 960–964.
- (22) (a) Parr, R. G.; Yang, W. *Density Functional Theory of Atoms and Molecules*; Oxford University Press: New York, 1988. (b) Ziegler, T. *Chem. Rev.* **1991**, *91*, 651–667.
- (23) (a) Ahlrichs, R.; Bär, M.; Häser, M.; Horn, H.; Kölmel, C. *Chem. Phys. Lett.* **1989**, *162*, 165–169. (b) Treutler, O.; Ahlrichs, R. *J. Chem. Phys.* **1995**, *102*, 346–354.
- (24) (a) Klamt, A.; Schürmann, G. *J. Chem. Soc., Perkin Trans.* **1993**, *2*, 799–805. (b) Schäfer, A.; Klamt, A.; Sattel, D.; Lohrenz, J. C. W.; Eckert, F. *Phys. Chem. Chem. Phys.* **2000**, *2*, 2187–2193.
- (25) (a) Schenk, C.; Schnepf, A. *Chem. Commun.* **2008**, *38*, 4643–4645. (b) Schenk, C.; Kracke, A.; Fink, K.; Kubas, A.; Klopfer, W.; Neumaier, M.; Schnöckel, H.; Schnepf, A. *J. Am. Chem. Soc.* **2011**, *133*, 2518–2524.
- (26) (a) Zintl, E. *Angew. Chem.* **1939**, *52*, 1–6. (b) Klemm, W. *Proc. Chem. Soc. London* **1959**, 329–341. (c) Busmann, E. Z. *Allg. Anorg. Chem.* **1961**, *313*, 90–106. (d) Kauzlarich, S. M. *Chemistry, Structure and Bonding of Zintl Phases and Ions*; VCH: New York, 1996.
- (27) (a) Wade, K. *Adv. Inorg. Chem. Radiochem.* **1976**, *18*, 1–67. (b) Mingos, D. M. P. *Nat. Phys. Sci.* **1972**, *236*, 99–102. (c) Mingos, D. M. P. *Acc. Chem. Res.* **1984**, *17*, 311–319.
- (28) King, R. B.; Silaghi-Dumitrescu, I.; Uță, M. M. *Eur. J. Inorg. Chem.* **2008**, 3996–4003.
- (29) Nava, P.; Sierka, M.; Ahlrichs, R. *Phys. Chem. Chem. Phys.* **2003**, *5*, 3372–3381.
- (30) Reed, A. E.; Weinstock, R. B.; Weinhold, F. *J. Chem. Phys.* **1985**, *83*, 735–746.
- (31) Mulliken, R. S. *J. Chem. Phys.* **1955**, *23*, 1833–1840.
- (32) (a) Boys, S. F. *Rev. Mod. Phys.* **1960**, *32*, 296–299. (b) Foster, J. M.; Boys, S. F. *Rev. Mod. Phys.* **1960**, *32*, 300–302.
- (33) Wang, J.-Q.; Stegmaier, S.; Wahl, B.; Fässler, T. F. *Chem.—Eur. J.* **2010**, *16*, 1793–1798.